Ligand exchanged photoluminescent gold quantum dots functionalized with leading peptides for nuclear targeting and intracellular imaging†

Shu-Yi Lin,[ac] Nai-Tzu Chen,[b] Shu-Pin Sum,[b] Leu-Wei Lo*[b] and Chung-Shi Yang*[ac]

Received (in Cambridge, UK) 14th May 2008, Accepted 27th June 2008
First published as an Advance Article on the web 8th August 2008
DOI: 10.1039/b808207c

Ligand exchanged gold quantum dots (GQDs) conjugated with cell-penetrating peptides are a new class of photoluminescent probes for nuclear targeting and intracellular imaging.

Gold nanoclusters such as nanospheres and nanorods have great potential in biological applications due to their small sizes, excellent biocompatibility and unique optical properties, including the well-characterized surface plasmon resonance (SPR) phenomena.[1–6] Gold nanoclusters have size-dependent SPR absorption in the visible wavelength range; decreasing their sizes into less than 3 nm will induce the disappearance of the SPR and the emergence of photoluminescence.[7–10] The photoluminescence quantum yields of gold nanoclusters can be enhanced by several orders of magnitude if their sizes are further decreased into the sub-nm scale.[11–13] This type of novel nanocluster, termed gold quantum dots (GQDs), have remarkable small size and excellent photoluminescent efficiency, which may be valuable properties toward their applicability in chemistry and biology.[14,15]

To prepare GQDs with high quantum yields, it is essential to manipulate the nucleation of gold within a well-defined molecular scaffold. For example, thiolate-protected GQDs can be prepared by chemical reduction of the complex formed from gold ions with alkanthiols, but the quantum yield is reduced because of their size-polydispersion since the gold core significant growth is influenced by the number of thiols.[16–18] Recently, polyamidoamine (PAMAM) dendrimer-encapsulated gold ions have been used to prepare GQDs with mono-dispersed size and excellent quantum efficiency.[11–13] Although the dendrimers are excellent molecular templates for the GQDs' formation, their safety concerns still remain to be clarified prior to biological application since it has been reported that they may exhibit cytotoxcity such as inducing haemolysis of human red blood cell.[19,20]

Herein we report a novel strategy utilizing 11-mercapto-undecanonic acid (MUDA) as a ligand to exchange GQDs (MUDA–GQDs) from PAMAM encapsulation before surface functionalization (Fig. 1). MUDA is a negatively charged thiol that exhibits strong interactions with gold and has been reported to have many fewer safety concerns.[21] MUDA is not only a protector to maintain the GQDs' stability in water, but also a building block to conjugate the GQDs with various biomolecules, for example, a specific peptide named SV40 nuclear-localization signal (NLS) which was used in the current study. Anchoring of such peptides on the sub-nm sized GQDs can facilitate their transport into the nucleus, assessable with the bright photoluminescence of the GQDs. The strategic synthesis and functionalization of the GQDs based on ligand exchange will become a prerequisite and an accessible method for extending their applications into various interestingly topics.

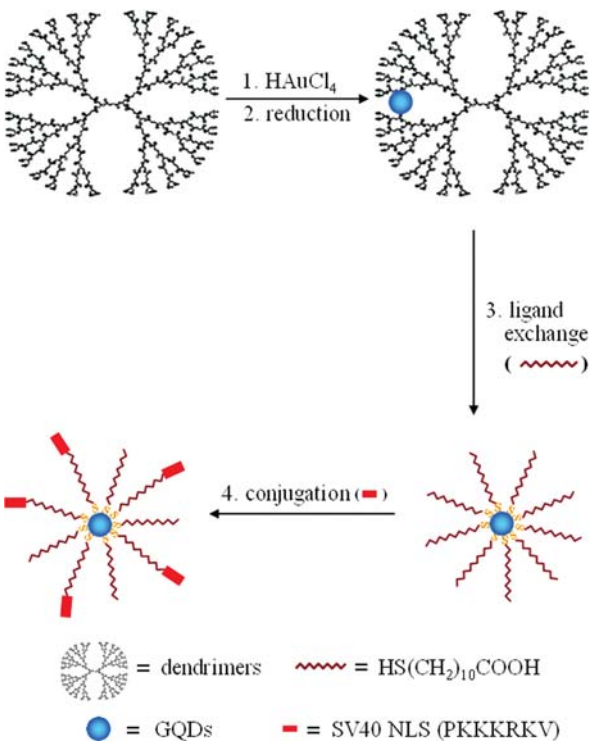

Fig. 1 Proposed strategy for GQDs synthesis, ligand exchange and derivatization.

[a] *Center for Nanomedicine Research, National Health Research Institutes, 35 Keyand Rd. Zhunan, Mialoli 350, Taiwan, R. O. C. E-mail: cyang@nhri.org.tw; Fax: 886-37-586447; Tel: 886-37-246-266 ext.38100*
[b] *Division of Medical Engineering Research, National Health Researches, Zhunan, Miaoli 350, Taiwan, R. O. C.*
[c] *Department of Applied Chemistry and Graduate Institute of Biomedicine and Biomedical Technology, National Chi-Nan University, Puli, Taiwan*

† Electronic supplementary information (ESI) available: Data including the detailed procedure for ligand exchange and cellular uptake. See DOI: 10.1039/b808207c

 This journal is © The Royal Society of Chemistry 2008

In this study, the fourth-generation of hydroxyl-terminated PAMAM dendrimer (G_4OH) containing blue-light emitting GQDs was synthesized at physiological temperature (37 °C) according to a previous method.[12] The 3 μmol gold ions ($HAuCl_4$, 0.2 wt% water solution) were added to 5 mL of deionized water containing 0.25 μmol G_4OH (10 wt% methanol solution). The solution was incubated in a cold room (4 °C) for 24 h until the gold ions were sequestered onto the G_4OH. Then the mixture was kept at 37 °C for 3 d to produce dendrimer-encapsulated GQDs. Fig. 2A shows the absorption sepctrum of the GQDs, which shows no SPR band at 520 nm (red line), indicating that the sizes of the GQDs are smaller than 1 nm. After introducing MUDA onto the GQDs, a similar absorption spectrum was observed (Fig. 2A, blue line), suggesting that the GQDs' sizes did not alter before and after the exchange. The GQDs exhibited photoluminescne with excitation and emission peaks at 370 nm and 450 nm (Fig. 2B, red line), respectively, which correspond to the published values.[12] Ligand exchange with MUDA did not appear to alter GQDs' photoluminescence excitation and emission wavelengths (Fig. 2B, blue line). These results suggest that the photoluminescent properties of the GQDs are unaffected by the ligand exchange.

MUDA–GQDs were purified by dialysis and dried by lyophilizer before transmission IR measurements. Fig. 3A and B show typical transmission IR spectra of MUDA alone and MUDA–GQDs, respectively. There are three significant differences in Fig. 3B when compared to Fig. 3A. First, as shown in the inset of the enlarged section between 2400 and 2650 cm^{-1}, the

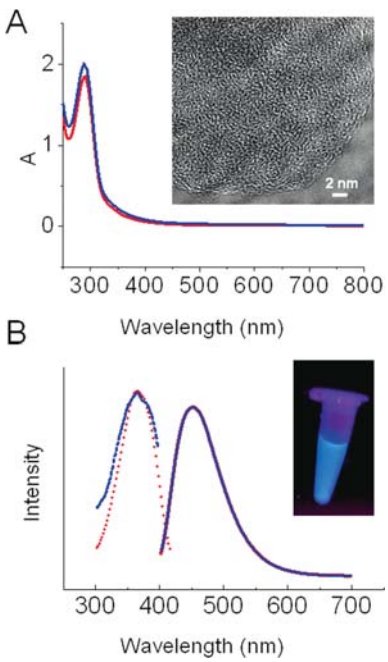

Fig. 2 Comparison of the optical properties of GQDs. (A) Absorption spectra of GQDs (red line) and MUDA–GQDs (blue line). (Inset) HRTEM image of MUDA–GQDs. The average core size of the GQD is less than 1 nm. (B) Corresponding photoluminescent spectra of the GQDs in (A), excitation (dashed line) and emission (solid line). (Inset) A color photo of the photoluminescence emission from MUDA–GQDs under UV lamp irradiation (366 nm).

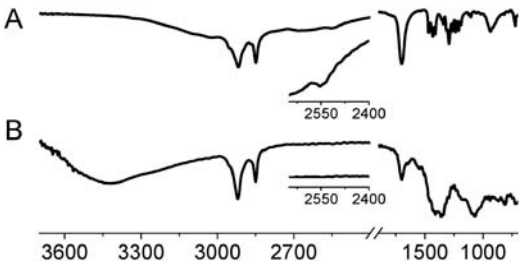

Fig. 3 Transmission FTIR spectra of dendrimer-encapsulated GQDs exchanged by MUDA. (A) MUDA alone and (B) MUDA–GQDs in a KBr pellet. The wavelengths for the magnified sections of (A) and (B) range from 2400 to 2650 cm^{-1}.

S–H stretch band around 2550 cm^{-1} is absent, resulting from the formation of the gold–sulfur bond. Second, the absorption at 3400 cm^{-1} is a result of residual moisture within the dried GQDs. Third, the peaks at 2919, 2850, 1700, 1560, 1410 and 1077 cm^{-1} are vibrational modes of $\upsilon_{asy}(CH_2)$, $\upsilon_{sym}(CH_2)$, $\upsilon_{str}(C{=}O)$, $\upsilon_{asy}(CO_2^-)$, $\upsilon_{sym}(CO_2^-)$ and υ_{str} (CO), respectively. These vibrational bands confirm the association of MUDA with GQDs.

To modify the MUDA–GQDs surface with NLS (NLS–MUDA–GQDs) for nuclear transport, 1-[(3-dimethylamino)-propyl]-3-ethylcarbodiimide hydrochloride (EDC) was then introduced to activate the carboxylic acid of MUDA before adding NLS. Fig. 4 shows photoluminescence images from the MUDA–GQDs (without NLS) and NLS–MUDA–GQDs

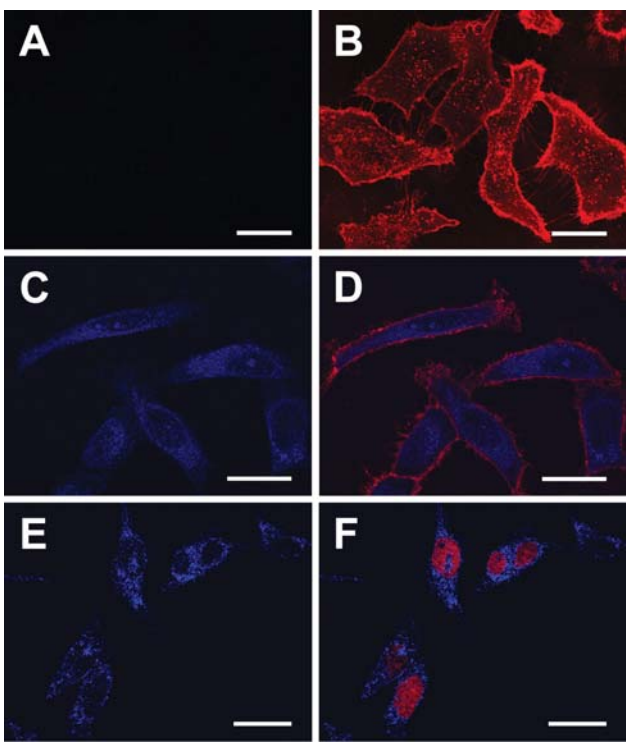

Fig. 4 Confocal microscope images of intracellular delivery of the GQDs. HeLa cells were treated by MUDA–GQDs (A and B) and NLS–MUDA–GQDs (E to F) for 1.5 h. The left panel shows the one-color image. The right panel shows the two-color colocalization image of the HeLa cells incubated with NLS–MUDA–GQDs were counterstained with a specific membrance dye (WGA–Alexa 594) and a nuclear dye (SYTO 59). Scale bar: 25 μm.

measured by the cofocal microscope, respectively. The one-color image shows no photoluminescent signal (panel A) from the cells treated with MUDA–GQDs, implying that MUDA–GODs were not able to enter the cells efficiently due to, at least in part, the negative surface-charge. On the contrary, intensive blue photoluminescence (panel C and E) from NLS–MUDA–GQDs were observed, indicative of the internalization of the MUDA–GQDs associated with NLS by HeLa cells. To illustrate the intracellular and nuclear distribution of NLS–MUDA–GQDs, the cells were counter-stained with a specific membrane dye, wheat germ agglutinin conjugated Alexa 594 (WGA-Alexa 594), and a nuclear dye, SYTO 59. The images of two-color colocalization (panel D and F) reveal that the blue photoluminescent signals from NLS–MUDA–GQDs are well-distributed within both the cytoplasm (panel D) and the nucleus (panel F), in comparison with the image of cells treated with MUDA–GODs (panel B) where only red fluorescence signals of WGA–Alexa 594 were observed. Therefore, the nuclear targeting of MUDA–GQDs are able to be achieved by the functionality of NLS, as shown in panel F with the two-color colocalization of images in the same confocal *z*-plane (blue: NLS–MUDA–GODs; red: SYTO 59).

To summarize, we have shown that GQDs can be exchanged by carboxylate-terminated *n*-alkanethiols such as MUDA from the dendrimer-template and further functionalized with site-specific leading peptides such as SV40 NLS. Additionally, we also show that GQDs can be applied as promising optical beacons for intracellular imaging and agents for subcellular targeting.

This work was supported by grants from the National Nanoscience and Nanotechnology Program of National Science Council (NSC-96-2120-M-260-001) and from the National Health Research Institutes (NHRI-MED-096-PP-04 and NHRI-096-NM-PP-03).

Notes and references

1 X. Shi, S. Wang, S. Meshinchi, M. E. V. Antwerp, X. Bi, I. Lee and J. R. Baker, Jr., *Small*, 2007, **3**, 1245.
2 A. K. Oyelere, P. C. Chen, X. Huang, I. H. El-Sayed and M. A. El-Sayed, *Bioconjugate Chem.*, 2007, **18**, 1490.
3 J. A. Dahl, B. L. Maddux and J. E. Hutchison, *Chem. Rev.*, 2007, **107**, 2228.
4 S. Eustis and M. A. El-Sayed, *Chem. Soc. Rev.*, 2006, **35**, 209.
5 C.-C. Chen, Y.-P. Lin, C.-W. Wang, H.-C. Tzeng, C.-H. Wu, Y.-C. Chen, C.-P. Chen, L.-C. Chen and Y.-C. Wu, *J. Am. Chem. Soc.*, 2006, **128**, 3709.
6 E. E. Connor, J. Mwamuka, A. Gole, C. J. Murphy and M. D. Wyatt, *Small*, 2005, **1**, 325.
7 T. K. Sham, P.-S. G. Kim and P. Zhang, *Solid State Commun.*, 2006, **138**, 553.
8 T. Shimizu, T. Teranishi, S. Hasegawa and M. Miyake, *J. Phys. Chem. B*, 2003, **107**, 2719.
9 T. Huang and R. W. Murray, *J. Phys. Chem. B*, 2001, **105**, 12498.
10 A. C. Templeton, S. Chen, S. M. Gross and R. W. Murray, *Langmuir*, 1999, **15**, 66.
11 J. Zheng, P. R. Nicovich and R. M. Dickson, *Annu. Rev. Phys. Chem.*, 2007, **58**, 409.
12 Y. Bao, C. Zhong, D. M. Vu, J. P. Temirov, R. B. Dyer and J. S. Martinez, *J. Phys. Chem. C*, 2007, **111**, 12194.
13 J. Zheng, C. Zhang and R. M. Dickson, *Phys. Rev. Lett.*, 2004, **93**, 077402-1.
14 C.-C. Huang, Z. Yang, K.-H. Lee and H.-T. Chang, *Angew. Chem., Int. Ed.*, 2007, **46**, 6824.
15 R. C. Triulzi, M. Micic, S. Giordani, M. Serry, W.-A. Chioue and R. M. Leblanc, *Chem. Commun.*, 2006, 5068.
16 Y. Negishi, K. Nobusada and T. Tsukuda, *J. Am. Chem. Soc.*, 2005, **127**, 5261.
17 J. P. Wilcoxon and J. E. Martin, *J. Chem. Phys.*, 1998, **108** 9137.
18 T. G. Schaaff, G. Knight, M. N. Shafigullin, R. F. Borkman and R. L. Whetten, *J. Phys. Chem. B*, 1998, **102**, 10643.
19 R. Duncan and L. Izzo, *Adv. Drug Delivery Rev.*, 2005, **57**, 2215.
20 D. M. Domanski, B. Klajnert and M. Bryszewska, *Bioelectrochemistry*, 2004, **63**, 189.
21 L. Ren, X.-L. Huang, B. Zhang, L.-P. Sun, Q.-Q. Zhang, M.-C. Tan and G.-M. Chow, *J. Biomed. Mater. Res. A*, 2008, **85**, 787.

 This journal is © The Royal Society of Chemistry 2008